FORUM ORIGINAL RESEARCH COMMUNICATION

High-Frequency Field Stimulation of Primary Neurons Enhances Ryanodine Receptor-Mediated Ca^{2+} Release and Generates Hydrogen Peroxide, Which Jointly Stimulate NF-κB Activity

Denise Riquelme,[1] Alvaro Alvarez,[1,*] Nancy Leal,[1,2,*] Tatiana Adasme,[1,*] Italo Espinoza,[1] Juan Antonio Valdés,[1,#] Natalia Troncoso,[1] Steffen Hartel,[4] Jorge Hidalgo,[1,2] Cecilia Hidalgo,[1,3] and M. Angélica Carrasco[1,2]

Abstract

Neuronal electrical activity increases intracellular Ca^{2+} concentration and generates reactive oxygen species. Here, we show that high frequency field stimulation of primary hippocampal neurons generated Ca^{2+} signals with an early and a late component, and promoted hydrogen peroxide generation via a neuronal NADPH oxidase. Hydrogen peroxide generation required both Ca^{2+} entry through N-methyl-D-aspartate receptors and Ca^{2+} release mediated by ryanodine receptors (RyR). Field stimulation also enhanced nuclear translocation of the NF-κB p65 protein and NF-κB -dependent transcription, and increased *c-fos* mRNA and type-2 RyR protein content. Preincubation with inhibitory ryanodine or with the antioxidant N-acetyl L-cysteine abolished the increase in hydrogen peroxide generation and the late Ca^{2+} signal component induced by electrical stimulation. Primary cortical cells behaved similarly as primary hippocampal cells. Exogenous hydrogen peroxide also activated NF-κB-dependent transcription in hippocampal neurons; inhibitory ryanodine prevented this effect. Selective inhibition of the NADPH oxidase or N-acetyl L-cysteine also prevented the enhanced translocation of p65 in hippocampal cells, while N-acetyl L-cysteine abolished the increase in RyR2 protein content induced by high frequency stimulation. In conclusion, the present results show that electrical stimulation induced reciprocal activation of ryanodine receptor-mediated Ca^{2+} signals and hydrogen peroxide generation, which stimulated jointly NF-κB activity. *Antioxid. Redox Signal.* 14, 1245–1259.

Introduction

NEURONAL ELECTRICAL ACTIVITY generates intracellular Ca^{2+} signals that induce local changes at the synaptic level, and activate at the nucleus the expression of genes that are essential for synaptic plasticity (11, 34). The activity-induced intracellular Ca^{2+} increase is a consequence of Ca^{2+} influx through different plasma membrane entry pathways, including Ca^{2+} channels activated by voltage or neurotransmitters and store-operated Ca^{2+} channels. In addition, there is a significant contribution from Ca^{2+} release through channels present in intracellular stores, mainly the endoplasmic reticulum (61, 89). Through Ca^{2+}-induced Ca^{2+} release (CICR), neuronal cells amplify and propagate small and localized Ca^{2+} signals generated in microdomains to other neuronal regions, including the nucleus (11, 20, 27, 58). Activation by Ca^{2+} of ryanodine receptors (RyR) or inositol 1,4,5-trisphosphate receptors (IP$_3$R) Ca^{2+} release channels provides the molecular basis for CICR.

Increased neuronal activity also produces reactive oxygen species (ROS) (13, 15, 31, 40), and reactive nitrogen species (RNS) (65). Numerous reports indicate that ROS at physiological concentrations act as requisite signaling molecules in processes underlying synaptic plasticity and memory formation (44, 46). Furthermore, mounting evidence supports crosstalk between Ca^{2+} and ROS signals (33, 39, 85). On the one hand, Ca^{2+} stimulates the production of ROS in different cell types, including neurons (2, 36, 48, 80). On the other, the redox state of the cell modifies the activity of several molecules involved in Ca^{2+} signaling, including the SERCA pump,

[1]Center of Molecular Studies of the Cell; Institute of Biomedical Sciences; Programs of [2]Physiology and Biophysics, [3]Cell and Molecular Biology, and [4]Anatomy and Developmental Biology, Faculty of Medicine, Universidad de Chile, Santiago, Chile.
*These authors contributed equally to the work.
#*Current affiliation:* Department of Biological Sciences, Faculty of Ecology and Natural Resources, Universidad Nacional Andres Bello, Santiago, Chile.

the IP$_3$R, and particularly the RyR channels. In skeletal muscle, the RyR1 isoform reversibly increases its activity after oxidation (4, 5, 28, 52, 69). In brain, the predominant RyR2 and RyR3 isoforms also increase their activity in response to oxidation, whereas after reduction they become poorly responsible towards activation by Ca^{2+} (17, 18, 37). In this context, our laboratory has reported that exogenous H$_2$O$_2$ applied to primary hippocampal cells or slices modifies the RyR redox state by increasing its *S*-glutathionylation level. This covalent and reversible RyR redox modification promotes Ca^{2+} release, which in turn enhances extracellular-signal related kinases 1/2 (ERK1/2) and cAMP response element-binding protein (CREB) phosphorylation (45).

Primary hippocampal cells exposed to electrical field stimulation at physiologically relevant frequencies display increased intracellular Ca^{2+} concentration due to Ca^{2+} influx through voltage-dependent Ca^{2+} channels (60). Calcium entry following neuronal stimulation activates caffeine-sensitive Ca^{2+} release from intracellular stores (6) and promotes mitochondrial-dependent superoxide anion generation (40). Increases in intracellular Ca^{2+} concentration or enhanced ROS generation activate the transcription factor NF-κB (32, 49, 57). This transcription factor plays a significant role in nerve cell survival, dendritic arborization, and axon formation and plasticity (3, 12, 35, 42, 43, 54, 56, 63, 76). Furthermore, depolarization by high extracellular K$^+$, low frequency stimulation (0.1 Hz), and long-term potentiation (LTP) induced by high frequency (HF) stimulation all promote NF-κB activation and enhance NF-κB-dependent expression in the hippocampus (30, 55, 57). Yet, to our knowledge, there are no reports in the literature describing the effects of HF field stimulation on NF-κB activity in primary neuronal cells.

The results described here show that electrical field stimulation of primary hippocampal neurons at physiologically relevant frequencies generated Ca^{2+} signals and promoted H$_2$O$_2$ generation, derived from a neuronal NADPH oxidase (NOX) activity. The generation of persistent Ca^{2+} signals and ROS required RyR-mediated Ca^{2+} release. The ensuing increase in Ca^{2+} and ROS jointly stimulated the translocation of the p65 NF-κB protein to the nucleus. In addition, after 6 h of HF stimulation neuronal cells displayed enhanced NF-κB-dependent transcription and increased RyR2 protein content, while 45 min after stimulation there was a sizable increase in the mRNA levels of the immediate early gene c-fos. Some experiments performed with cortical cells obtained from the medial prefrontal area yielded similar results as those obtained in primary hippocampal cells.

Materials and Methods

Materials

Dulbecco's modified Eagle's medium (DMEM), N-acetyl-L-cysteine (NAC), uridine, and antibodies anti-β-actin, anti-microtubule-associated protein 2 (MAP-2), and MK-801 were obtained from Sigma (St. Louis, MO). Ryanodine was from Alexis (San Diego, CA) and H$_2$O$_2$ from Merck (Darmstadt, Germany). Diphenylene iodonium (DPI) and protease inhibitors were from Calbiochem (La Jolla, CA). Lipofectamine 2000, Hoechst 33342, SYBR green (Platinum SYBR Green qPCR SuperMix UDG), and B27 were from Invitrogen (Carlsbad, CA). Horse serum, Neurobasal and Full Neurobasal medium were from Gibco BRL (Rockville, MD). BAPTA-AM,

Fluo-4-AM, Alexa Fluor 546 goat anti-rabbit IgG, and Alexa Fluor 488 goat anti-mouse IgG were from Molecular Probes (Eugene, OR). The peptides gp91 ds-tat and scrambled-tat were from AnaSpec (Fremont, CA). Anti-glial fibrillary acidic protein (GFAP) was from Dako (Carpinteria, CA). The antibody against NF-κB inhibitory alpha (IκBα) was from Cell Signaling Technology (Beverly, MA). Antibody anti-RyR2 and secondary horse rabbit peroxidase-conjugated anti-rabbit antibody were from Pierce (Rockford, IL). Polyvinylidine difluoride membranes were from Millipore Corp, (Bedford, MA).

Primary cell cultures

All experimental protocols used in this work complied with the "Guiding Principles for Research Involving Animals and Human Beings" of the American Physiological Society and were approved by the Bioethics Committee for Investigation in Animals of the Facultad de Medicina, Universidad de Chile.

Hippocampal neurons were obtained from Sprague–Dawley rats at embryonic day 18. The hippocampus was dissected, and primary cultures were prepared as described previously (19). Cells were seeded in polylysine-coated plates or in 25 mm coverslips and maintained for 2 h in DMEM supplemented with 10% horse serum; after this time, cells were transferred to Neurobasal medium supplemented with B27, 100 μg/ml streptomycin, and 100 U/ml penicillin (Full Neurobasal). To reduce the number of proliferating non-neuronal cells, cultures were treated at 3 days *in vitro* (DIV) with 1.4 ng/μl 5-Fluoro-2′-deoxy-uridine (FDU) plus 3.5 ng/μl uridine for 24 h. For most of the assays, cells were seeded at 5×10^4 cells/cm^2 and treatments were performed at 10–14 DIV. The neuronal content of these cultures was assessed by immunocytochemistry, using MAP-2 as neuronal marker and GFAP as glial marker. At day 14, DIV the culture contained at least 80% neurons (Supplemental Fig. 1A; *see* www.liebertonline.com/ars).

Cortical neurons were obtained from the medial prefrontal cortex from E18 rat fetuses. The same procedure used to obtain hippocampal cultures was followed. Cells were used at 6–10 DIV.

Repetitive field electrical stimulation

Primary cell cultures were kept in Tyrode solution (in mM: 129 NaCl, 5 KCl, 2 CaCl$_2$, 1 MgCl$_2$, 30 glucose, 25 HEPES-Tris, pH 7.3) under resting conditions for 30 min. For experiments in Ca^{2+}-free Tyrode solution, CaCl$_2$ was replaced by 2 mM MgCl$_2$ and 0.5 mM EGTA was added. To elicit action potentials, electrical field stimulation of 20–25 V/cm was applied through platinum wires located in the microscope field of view, using 1 ms supra-threshold voltage pulses delivered from high current capacity stimulators. Neurons were stimulated with 1 or 4 trains of 1000 pulses at 50 or 10 Hz. Drugs were added to Tyrode solution, when used, before electrical stimulation or the addition of H$_2$O$_2$ for the times described in each case.

The electrical stimulation protocols used in this work did not produce neuronal death, as evaluated 1, 6, and 24 h after the stimulus by immunocytochemistry of MAP2-stained neurons loaded with propidium iodide. Supplemental Fig. 1B illustrates an example of a primary hippocampal culture stimulated with 4000 pulses at 50 Hz and evaluated for viability 24 h later.

Determination of H_2O_2 generation

Hippocampal and cortical neurons were transiently transfected with the Hyper™-Cyto plasmid (Evrogen, Moscow, Russia) at 9 or 6 DIV, respectively. This plasmid codes for a cytoplasmic protein (HyPer-cyto), which has a circularly permuted yellow fluorescent protein inserted into the regulatory domain of the prokaryotic H_2O_2-sensing protein (OxyR) (10) allowing selective detection of H_2O_2 production in living cells. The efficiency of neuronal transfection was 11%. One day post-transfection, cells were washed with Tyrode solution and electrically stimulated in the same solution.

Images were obtained every 10 s with an Olympus Disk Scanning Unit (DSU) confocal microscope (Olympus, Hamburg, Germany). Hyper™-Cyto fluorescence was detected at 488 nm excitation and 510–540 nm emission wavelengths. Changes in H_2O_2 levels are presented as $(F-F_o)/F_o$ values, where F_o corresponds to the average basal fluorescence obtained from 15 frames.

Detection of intracellular Ca^{2+} signals

Cells were transferred to Tyrode solution, preloaded for 30 min at 37°C with 5 μM Fluo4-AM and washed three times with Tyrode solution to allow complete dye de-esterification. Fluorescence images of intracellular Ca^{2+} signals in primary hippocampal neurons were acquired every 5 s in an inverted confocal microscope (Carl Zeiss, Axiovert 200, LSM 5 Pascal, Jena, Germany), utilizing the Plan Apochromatic 40× Oil DIC objective, at excitation 488 nm, argon laser beam. Most image data were acquired in cell bodies. Frame scans were averaged using the equipment data acquisition program. Ca^{2+} signals are expressed as $(F-F_{min})/(F_{max}-F)$, where F corresponds to the experimental fluorescence, F_{max} to the fluorescence signal of Ca^{2+}-satured dye, and F_{min} to the fluorescence of Ca^{2+}-free dye. The values of F_{max} and F_{min} were determined at the end of experiment; F_{max} after ionophore addition (ionomycin, 100 μg/ml) and F_{min} after addition of 100 μM BAPTA as Ca^{2+}-chelator. All experiments were performed at room temperature (20°–22°C).

Immunoblot analysis

Cells were incubated at 4°C in 30 μl lysis buffer containing (in mM) 150 NaCl, 1 EDTA, 5 Na_3VO_4, 20 NaF, 10 $Na_4P_2O_7$, 50 Tris-HCl, pH 7.4, plus 1% Nonidet P-40 and protease inhibitors as described Valdés et al., (83). Cell lysates were scrapped from the culture dishes, disrupted by sonication for 1 min, incubated on ice for 20 min, and sedimented at 15,000 g for 20 min to remove debris. Whole cell lysates were resolved by 10% SDS-PAGE. Gels were transferred to 0.2 μm polyvinylidine difluoride membranes, and blots were blocked for 1 h at room temperature in TBS containing 0.1% Tween-20 and 5% fat-free milk. Incubations with primary antibody against IκBα (1:500) were performed at 4°C overnight. After incubation for 1.5 h with HRP-conjugated secondary antibodies, membranes were developed by enhanced chemiluminescence (Amersham Biosciences, Bath, UK). The films were scanned and the Image J program was employed for densitometric analysis of the bands. To correct for loading, membranes were stripped and blotted against β-actin.

Detection and quantification of RyR2 protein content in immunoblots was carried out as described in detail elsewhere (16).

Plasmid constructs

A plasmid containing six tandem repeats of NF-κB binding sites linked to a luciferase reporter gene (pGL3, Promega, Madison, WI) was constructed (83). Briefly, the plasmid was produced using six copies of consensus sequences inserted immediately upstream of the pGL3 promoter (Xho I site). The orientation of the insert was verified by PCR amplification of the isolated DNA of the different clones. Full-length p65 was subcloned from p65-GFP (62) into the pEGFP-N1 vector (Clontech, Mountain View, CA) using HindIII and BamHI restriction sites (83).

Reporter gene transient transfection and luciferase reporter assay

Cells in primary culture were transiently transfected with Lipofectamine 2000 (Invitrogen) according to the manufacturer's specifications. Neurons were transfected with 3 μl Lipofectamine-2000 in 100 μl Neurobasal medium containing 0.9 μg of the reporter vector DNA (6X NF-κB -pGL3), and 0.1 μg of the Renilla phRL-TK vector (Promega). Transfection efficiency was 16%, evaluated with an enhanced green fluorescent protein (eGFP) protein expression vector (Clontech), and calculated as the percentage of the fluorescence-emitting cells relative to the total number of cells.

One day post-transfection, cultures were electrically stimulated with varying protocols as described in the text. Cells were lysed 6 h after stimulation; at this particular time, the maximum response of luciferase activity was obtained. Luciferase activity was determined using a Dual-luciferase reporter assay system (Promega); a Berthold F12 luminometer was used for light detection. Results, normalized for transfection efficiency, are expressed as the ratio of firefly to Renilla luciferase light emission.

Visualization of p65–eGFP in neuronal cells by confocal microscopy

Hippocampal neurons were plated over polylysine-coated 60 mm plates with 10 coverslips at 50,000 cells/cover. Cultures were transiently transfected with vector eGFP or p65–eGFP, at 7 or 8 DIV. Cells electrically stimulated in Tyrode medium were fixed with 4% paraformaldehyde in PBS solution. Nuclei were stained with 5 μg/ml Hoechst 33342. Coverslips were mounted and analyzed by confocal microscopy (Carl Zeiss, Axiovert 200, LSM 5 Pascal, Jena, Germany) under the following conditions: intensity I∈ [0, 255], X63 oil objective, NA 1.4, excitation/emission 488/505–530 nm for GFP or p65–eGFP. For image deconvolution, confocal raw-images were analyzed using the Huygens Scripting (Scientific Volume Imaging, Hilversum, Netherlands) commercial software. The image-processing routines developed elsewhere (71) for visualization, segmentation of regions of interest (ROIs), and for calculation of intensities and areas based on Interactive Data Language (ITT, Boulder, CO), were employed.

All image acquisition, deconvolution, and image processing routines remained constant along comparative experiments, and the quality of the segmentation was controlled iteratively by overlaying the original fluorescent images with the mask in each channel.

The levels of *c-fos* mRNA were analyzed by semiquantitative RT-PCR as previously described (21). RyR2 mRNA levels were quantified both by semiquantitative RT-PCR and by real-time PCR by using the primers described in Zhao *et al*. (86). Briefly, real-time quantitative PCR (qRT-PCR) was performed in a MX3000P thermocycler (Stratagene, Garden Grove, CA) using the DNA binding dye SYBR. Levels of RyR2 and β-actin were determined by the 2-$\Delta\Delta$CT method (70). Dissociation curves were analyzed to verify purity of products. All samples were analyzed at least in triplicate.

Statistics

Results are expressed as mean ± SEM. The significance of differences was evaluated using Student's *t*-test for paired data, and one-way or two-way ANOVA followed by Bonferroni's post-test for multiple determinations, as indicated.

Results

In this work, we studied in primary neurons the effects of HF electrical stimulation on cytoplasmic Ca^{2+} signals and ROS generation, and on the activity of the transcription factor NF-κB. We used protocols of varying intensity (1000 to 4000 pulses, 10 or 50 Hz) to stimulate mainly primary hippocampal neurons, albeit we performed some experiments in neurons obtained from the medial prefrontal cortical area of rat brain. The hippocampus sends efferent projections to this cortical area and hippocampal stimulation produces paired pulse facilitation and LTP (84). After 10-DIV, primary cortical and hippocampal neurons displayed resting membrane potentials ranging around −60 mV (measured in Tyrode medium) and substantial synaptic activity, detected in the form of either excitatory post-synaptic potentials or currents.

ROS generation after electrical stimulation of primary neurons requires RyR-mediated Ca^{2+} release and NADPH oxidase activity

To detect ROS generation, we transfected primary neurons with the Hyper™-Cyto plasmid (pHyPer-cyto). This mammalian expression vector encodes the cytoplasmic fluorescent sensor protein HyPer (HyPer-cyto), which specifically senses H_2O_2 and does not present autofluorescence (10). Primary hippocampal neurons responded to field electrical stimulation (1 train, 1000 pulses, 50 Hz) with a significant increase in probe fluorescence over time, as illustrated by the averaged
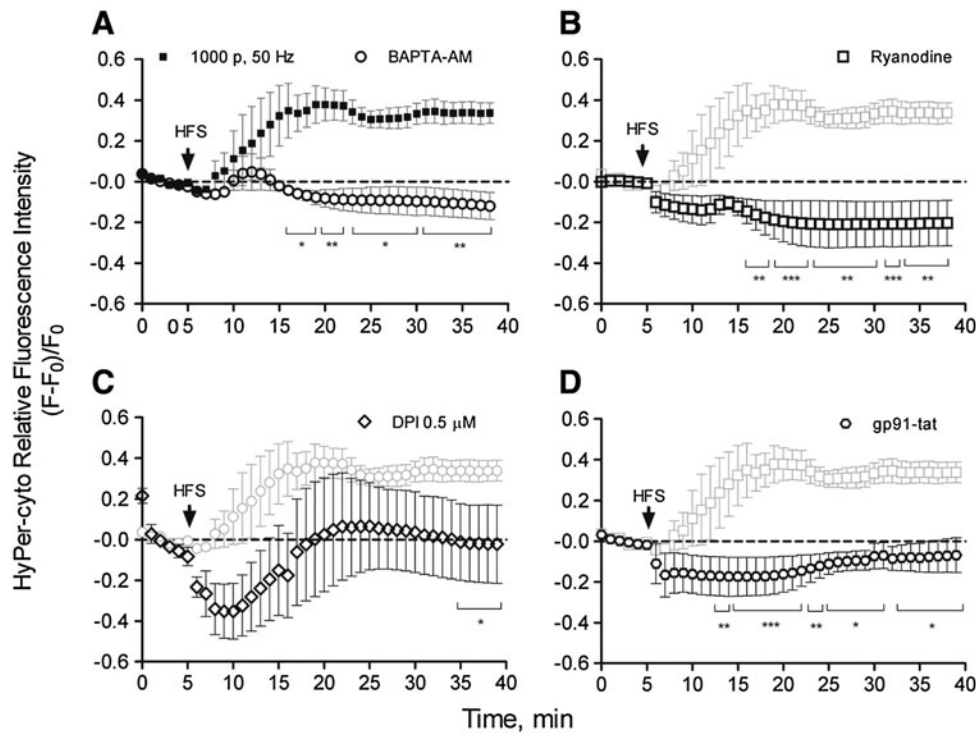

FIG. 1. ROS generation in electrically stimulated hippocampal neurons. Primary hippocampal cells were transfected with the Hyper™-Cyto plasmid. After 24 h, cell cultures were stimulated with 1000 pulses at 50 Hz (HFS, indicated by *arrows*). Probe fluorescence was collected from neuronal cytoplasmic ROI. (**A**) *Black solid symbols* represent the fluorescence collected from neurons in control conditions ($n = 8$), and *open symbols* from cells preincubated with 100 μM BAPTA-AM to chelate intracellular Ca^{2+} ($n = 3$). (**B**) *Black open symbols* represent the fluorescence collected from neurons preincubated for 1 h with 50 μM ryanodine, and stimulated in the presence of ryanodine ($n = 3$). In this and subsequent graphs (**C** and **D**), the *light gray symbols* correspond to the fluorescent values collected from the control cells shown in **A**. (**C**) *Black open symbols* represent the fluorescence collected from neurons preincubated for 30 min with 0.5 μM DPI ($n = 3$). (**D**) *Black open symbols* represent the fluorescence collected from neurons preincubated for 1 h with 1 μM gp91 ds tat ($n = 3$). All data represent mean ± SEM. Statistical significance of mean differences (**A, B, D**) was evaluated by two-way ANOVA followed by Bonferroni's post-test. Results in **C** were evaluated by Student's *t* test. *p < 0.05, **p < 0.01, ***p < 0.001.

results shown in Figure 1A. Probe fluorescence peaked 10 min after stimulation and remained elevated for the following 25 min, at which point recording stopped. Supplemental Figure 2A (*see* www.liebertonline.com/ars) illustrates a particular example recorded in a primary hippocampal culture. Primary cortical neurons also displayed a significant increase in HyPer-cyto fluorescence after HF (1000 pulses, 50 Hz) electrical stimulation, (Supplemental Fig. 2B). Preincubation with 10 mM N-acetyl-L-cysteine (NAC) abolished this ROS increase in primary cortical and hippocampal neurons (Supplemental Figs. 2C and 2D).
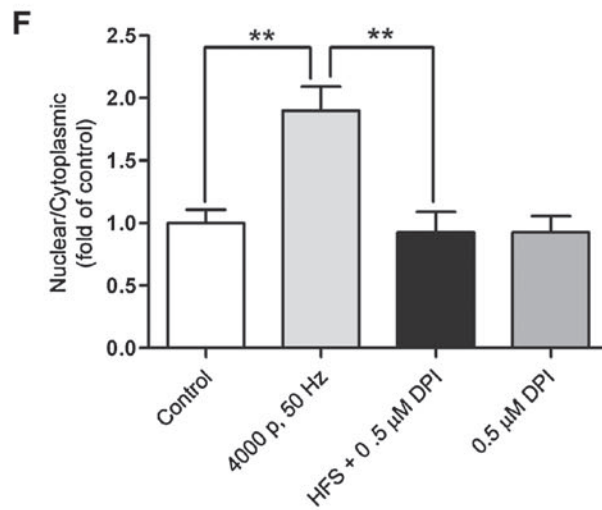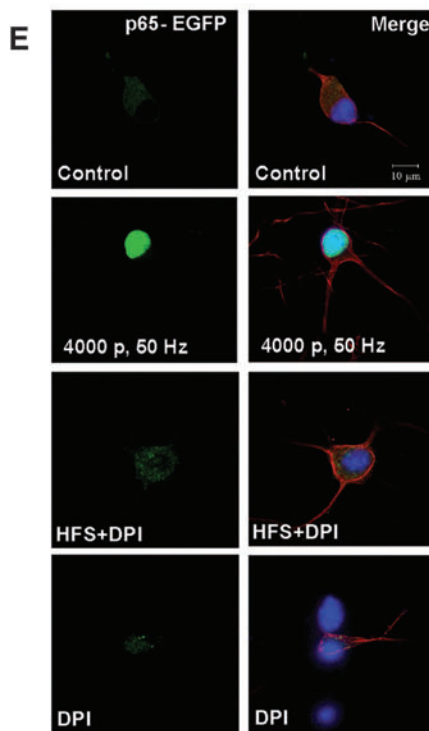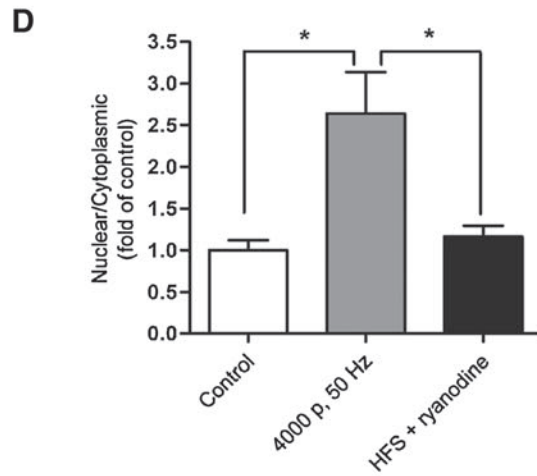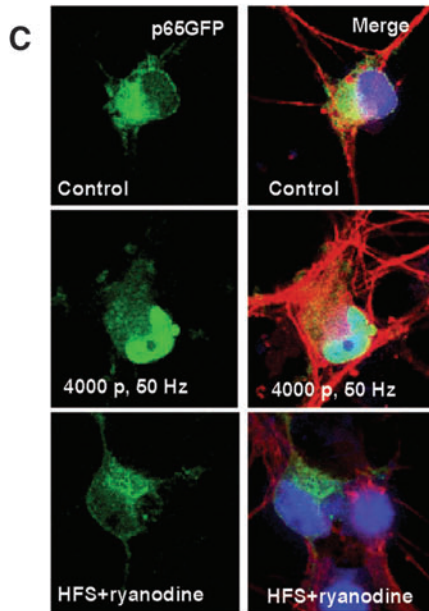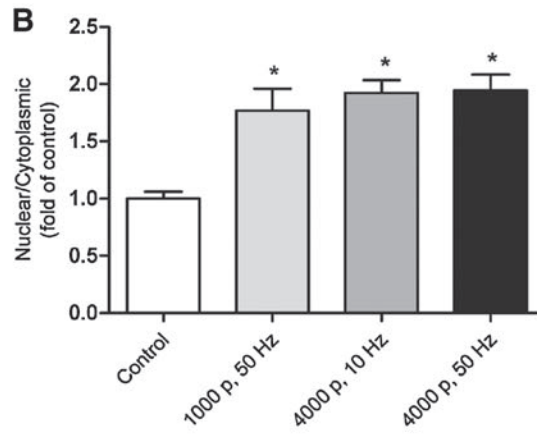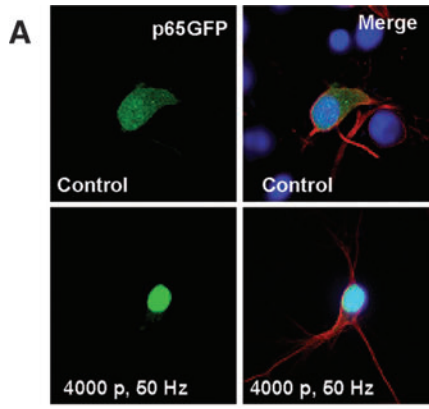
The ROS increase induced by electrical stimulation (1000 pulses, 50 Hz) was calcium dependent since it did not occur in hippocampal neurons preincubated with 100 μM BAPTA-AM (Fig. 1A). This concentration of BAPTA-AM completely prevented the increase in cytoplasmic Ca^{2+} concentration produced by electrical stimulation (data not shown). Likewise, hippocampal cells preincubated for 60 min with 50 μM ryanodine, a condition that completely prevents RyR-mediated Ca^{2+} release in these cells (45), did not present an increase in H_2O_2 following electrical stimulation but displayed somewhat lower probe fluorescence than prior to stimulation (Fig. 1B). Preincubation of primary hippocampal cultures with MK801, an inhibitor of N-methyl D-aspartate (NMDA) receptor activity (15, 31) not only abolished the fluorescence increase produced by electrical stimulation (1000 pulses, 50 Hz) but caused a sizable decrease in probe fluorescence after a few minutes (Supplemental Fig. 3A; *see* www.liebertonline.com/ars). Together, these observations strongly suggest that H_2O_2 generation induced by electrical stimulation requires Ca^{2+} and that the main Ca^{2+} source is of intracellular origin, supplied via RyR-mediated Ca^{2+}-induced Ca^{2+} release (CICR) caused by Ca^{2+} entry through NMDA receptors.

The main source of ROS generation after electrical stimulation of primary neurons is NADPH oxidase

Previous reports indicate that hippocampal neurons possess a NOX activity that generates superoxide anion (82). Superoxide anion is a labile free radical that readily dismutates into H_2O_2. To test the possible contribution of NOX as a source of H_2O_2, we preincubated cells with 10 μM DPI to inhibit flavin-containing enzymes such as NOX that catalyze ROS formation (1, 2). Preincubation of hippocampal neurons with 10 μM DPI prevented the increase in fluorescence produced by electrical stimulation (1 train, 1000 pulses, 50 Hz) and caused a sizable and transient decrease in probe fluorescence right after stimulation (Supplemental Fig. 3B). As illustrated in Figure 1C, a lower concentration of DPI (0.5 μM) that inhibits exclusively NOX activity (1) produced a similar response. Furthermore, as shown in Figure 1D, cells incubated with gp91ds-tat, an inhibitory peptide of NOX activity that prevents NOX assembly (74), did not generate H_2O_2 in response to electrical stimulation (1000 pulses, 50 Hz). In contrast, hippocampal cells incubated with a scrambled peptide of gp91-tat (scramb-tat), presented similar ROS generation in response to electrical stimulation as controls (Supplemental Fig. 3C). All combined, these results strongly suggest that NOX is the main source of the calcium-dependent H_2O_2 generation displayed by primary hippocampal cells in response to HF electrical stimulation.
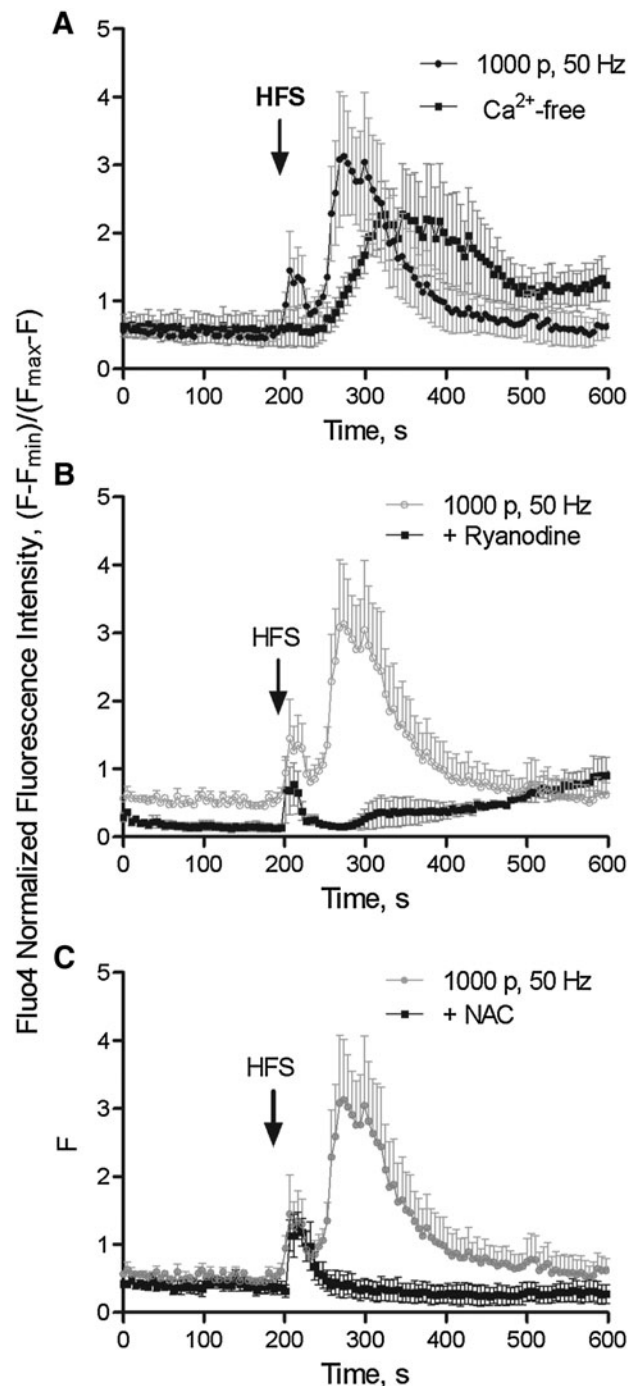
FIG. 2. Calcium signals induced by electrical stimulation in hippocampal neurons. Hippocampal cells preloaded for 30 min at 37°C with 5 μM Fluo4-AM were stimulated with 1000 pulses at 50 Hz. (**A**) *Solid circles* represent the fluorescence collected from neurons in control conditions ($n = 5$), and *solid triangles* from cells stimulated in Ca^{2+}-free solution ($n = 3$). (**B**) *Black solid symbols* represent the fluorescence collected from neurons preincubated for 1 h with 50 μM ryanodine, and stimulated in the presence of ryanodine ($n = 3$). (**C**) *Black solid symbols* represent the fluorescence collected from neurons preincubated for 1 h with 10 mM NAC ($n = 3$). A Student's *t*-test analysis of the results obtained for the first Ca^{2+} peak in control conditions and after treatment with NAC did not result in significant differences. In **B** and **C**, the *light gray symbols* correspond to the control cells shown in **A**.

Calcium signals in hippocampal primary neurons exposed to electrical stimulation

Electrical stimulation (1000 pulses, 50 Hz) of primary hippocampal cultures loaded with Fluo4-AM produced an immediate increase in probe fluorescence, followed by a second larger signal (Fig. 2). Only the first signal remained, albeit reduced, in cultures preincubated with inhibitory ryanodine, as illustrated by the single experiment shown in Figure 2A and the averaged data shown in Figure 2B. Preincubation with NAC for 1 h also abolished the second Ca^{2+} signal, while the first signal was not significantly different to the control (Fig. 2C). A stronger stimulation protocol (4 trains of 1000 pulses, 50 Hz) elicited transient Ca^{2+} signals during each stimulation train, followed by a second Ca^{2+} signal of extended duration; preincubation with 50 μM ryanodine or 10 mM NAC abolished all Ca^{2+} signals (Supplemental Fig. 4; *see* www.liebertonline.com/ars).

Electrical stimulation promotes NF-κB translocation to the nucleus; this process requires both RyR-mediated Ca^{2+} release and ROS generation

The regulated translocation of NF-κB to the nucleus is a requisite step for the activation of this transcription factor. Of the several NF-κB proteins expressed in neurons, we chose to study the translocation of the ubiquitous p65 component, which is present in hippocampal cells (57). We performed experiments in hippocampal neurons transfected with p65–eGFP and studied by confocal microscopy its translocation to the nucleus in response to different electrical stimulation protocols. In addition, we investigated if p65 translocation to the nucleus required Ca^{2+}, in particular RyR-mediated Ca^{2+} release from intracellular stores, and ROS generation.

Stimulation with four consecutive trains of 1000 pulses each at 50 Hz produced significant translocation of the p65–eGFP fluorescent probe to the nucleus, as visualized by confocal microscopy (Fig. 3A). Weaker HF stimulation protocols (4000 pulses, 10 Hz, or 1000 pulses, 50 Hz) produced comparable effects (Fig. 3B).

To investigate whether RyR-mediated Ca^{2+} release participates in p65 translocation, hippocampal cells preincubated for 1 h with 50 μM ryanodine were stimulated with 4 trains of 1000 pulses, at 50 Hz. As shown by the fluorescent microscopy images illustrated in Figure 3C, p65–eGFP translocation to the nucleus required functional RyR, since cells preincubated with ryanodine showed values of p65–eGFP translocation similar to those exhibited by controls (Figs. 3C and 3D).

To determine whether NOX-generated ROS participate in p65 translocation to the nucleus, cells were exposed to the same electrical stimulation protocol (4 trains of 1000 pulses, 50 Hz) in the presence of 0.5 μM DPI to inhibit NOX selectively. DPI-treated cells exhibited the same translocation as control cells or cells incubated with DPI but not stimulated (Figs. 3E and 3F).

Taken together, these results strongly suggest that p65 translocation to the nucleus elicited by HF electrical stimulation of primary hippocampal cells requires RyR–mediated Ca^{2+} release and NOX generated ROS.

We tested next the effects on p65 translocation of 10 μM DPI as a general inhibitor of flavin-containing proteins, and of 10 mM NAC as universal ROS scavenger, since as stated above, these two agents completely inhibited H_2O_2 generation in response to electrical stimulation of primary neurons. Both DPI (Fig. 4A) and NAC (Fig. 4B) completely prevented the translocation of p65–eGFP in cells electrically stimulated (4 trains of 1000 pulses, 50 Hz). As illustrated in Figure 4C, NAC also prevented the enhanced p65 translocation induced by a milder electrical stimulation protocol (1000 pulses, 10 Hz). These results confirm that p65 translocation induced by electrical stimulation requires an elevation in intracellular ROS levels.

Exogenous H$_2$O$_2$ stimulates NF-κB activity in primary hippocampal and cortical neurons

As detailed above, hippocampal cells display significantly enhanced H_2O_2 generation after electrical stimulation. For this reason, we analyzed the effects of exogenous H_2O_2 on NF-κB activity in resting neurons. Hippocampal neurons exposed to 200 μM H_2O_2 for 5 min showed a significant increase in NF-κB activity, assayed with a reporter gene (Fig. 5A), and a concomitant decrease in IκBα levels (Fig. 5B). In addition, RyR inhibition with ryanodine drastically reduced the increase in NF-κB-dependent transcription induced by H_2O_2 in hippocampal neurons to levels comparable to those of control cells

FIG. 3. Translocation of p65 to the nucleus in electrically stimulated hippocampal neurons. Cultured hippocampal neurons transfected with p65–eGFP were electrically stimulated with different protocols. When specified, cultures were preincubated with ryanodine or DPI, and these agents were also present during and after HF stimulation. Cultures were fixed 90 min after the HF stimulus and analyzed for subcellular NF-κB p65–eGFP (*green*) distribution. Nuclei were stained with Hoechst (*blue*) and neurons with MAP-2 (*red*). Fluorescence images from 10 to 15 neurons in each experimental condition were collected by confocal microscopy as described in detail in the text. (**A**) Fluorescent microscopy images collected from hippocampal cells under control conditions (*upper panels*) or after stimulation with 4000 pulses at 50 Hz (*lower panels*). (**B**) Quantification of p65–eGFP distribution into nucleus and cytoplasm in control conditions and in cells exposed to three different electrical stimulation protocols. (**C**) Fluorescent microscopy images of hippocampal cells under control conditions (*upper panels*), after stimulation with 4000 pulses at 50 Hz (*mid panels*), or after stimulation with 4000 pulses at 50 Hz in the presence of 50 μM ryanodine (*lower panels*). (**D**) Quantification of p65–eGFP distribution into nucleus and cytoplasm under control conditions, after 4000 pulses at 50 Hz, and after stimulation in the presence of 50 μM ryanodine. (**E**) Fluorescent microscopy images collected from hippocampal cells under control conditions (*first row*), after stimulation with 4000 pulses at 50 Hz (*second row*), after stimulation with 4000 pulses at 50 Hz in the presence of 0.5 μM DPI (*third row*), and after preincubation for 30 min with 0.5 μM DPI (*fourth row*). (**F**) Quantification of p65–eGFP distribution into nucleus and cytoplasm under control conditions, after stimulation with 4000 pulses at 50 Hz, after this same HF stimulation in the presence of 0.5 μM DPI, and after preincubation with 0.5 μM DPI. Data in **B**, **D** and **F** represent mean $\pm$ SEM of the fluorescence ratio nucleus/cytoplasm from three independent experiments. Statistical significance was evaluated by one-way ANOVA followed by Bonferroni's post-test. *$p < 0.05$, **$p < 0.01$.

(Fig. 5A). Taken together, these results suggest that H_2O_2 activates the NF-κB pathway by stimulating IκBα degradation, and that the increase in NF-κB reporter activity induced by H_2O_2, which involves IκBα degradation, requires functional RyR to supply Ca^{2+} via RyR-mediated Ca^{2+} release.
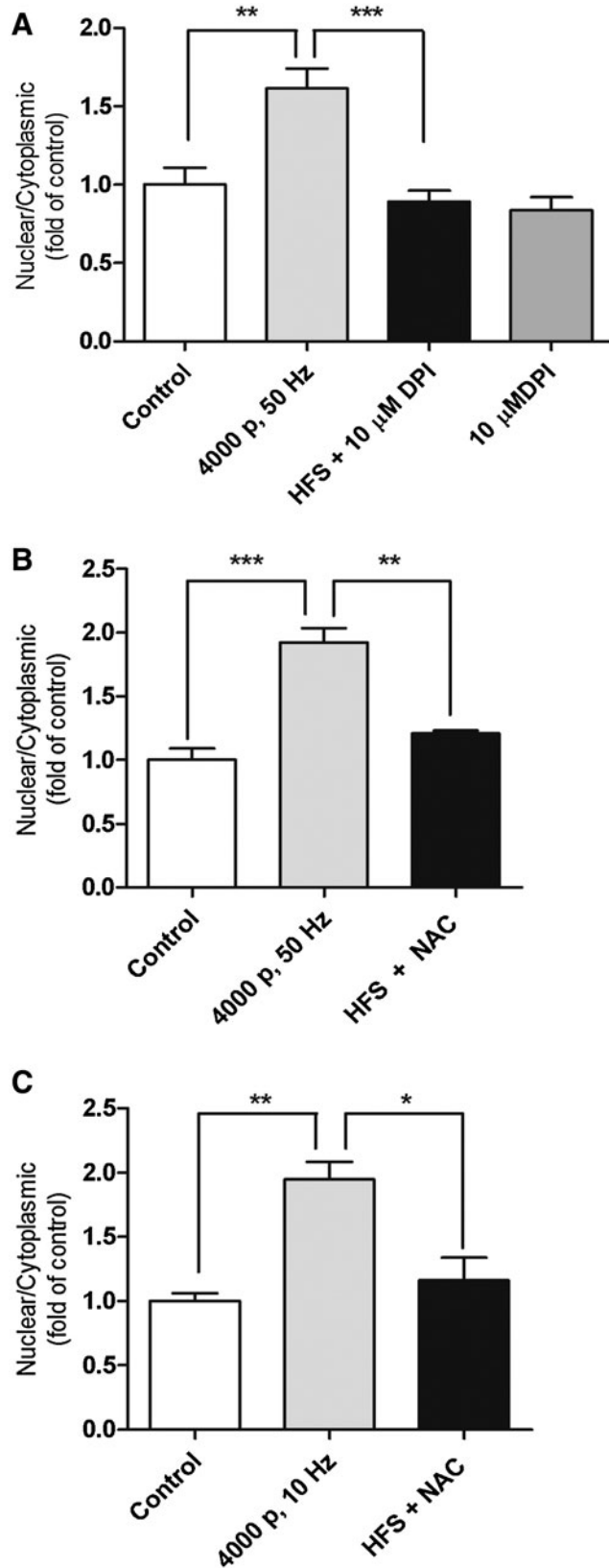
We studied cortical neurons under the same conditions employed for hippocampal neurons, except for the fact that cortical cells were transfected with the NF-κB reporter gene at 6 DIV. We found that exogenous H_2O_2 also stimulated the NF-κB pathway in cortical neurons, as determined through the activation of the NF-κB reporter gene (Fig. 5C) and decreased IκBα levels (Fig. 5D).

Electrical stimulation promotes NF-κB activity in primary hippocampal and cortical neurons

We assayed the effects of different electrical stimulation protocols (1000 or 4000 pulses, 10 or 50 Hz) on NF-κB activity in hippocampal or cortical neurons transfected with a NF-κB reporter gene. As shown in Figure 6A, hippocampal neurons showed a statistically significant 2-fold increase in reporter activity after three different stimulation protocols (1000 pulses, 10 Hz, 4 trains of 1000 pulses, 10 or 50 Hz). Parallel experiments in hippocampal cells stimulated with 4 trains of 1000 pulses, at 50 Hz, showed significantly reduced IκBα levels (Fig. 6B), to levels comparable to those displayed by hippocampal cells exposed to exogenous H_2O_2 (Fig. 5B).

Cortical cells showed a significant increase in NF-κB reporter gene activity in response to stimulation with 4 trains of 1000 pulses at 50 Hz. Other stimulation protocols showed a tendency to increase reporter gene activity but without reaching statistical significance (Fig. 6C).

Electrical stimulation enhances c-fos expression and increases RyR2 protein content in primary hippocampal neurons

HF stimulation (4000 pulses, 50 Hz) of primary hippocampal neurons increased >2-fold the mRNA levels of the immediate early gene c-fos, measured 45 min after stimulation (Supplemental Fig. 5; *see* www.liebertonline.com/ars). In addition, this stimulation protocol produced a significant increase in RyR2 protein content, measured after

FIG. 4. **Effects of DPI or NAC on p65 translocation to the nucleus induced by field electrical stimulation of primary hippocampal neurons.** Cultured hippocampal neurons transfected with p65–eGFP were electrically stimulated with different protocols. When specified, cultures were pre-incubated with 10 μM DPI or 10 mM NAC for 30 min or 1 h, respectively, and these agents were maintained during and after HF stimulation. Cultures were fixed 90 min after the HF stimulus and analyzed for subcellular NF-κB p65–eGFP distribution into nucleus and cytoplasm. Fluorescence was determined in 10 to 15 neurons in each experimental condition. (**A**) Quantification of p65–eGFP under control conditions, after stimulation with 4000 pulses at 50 Hz, after stimulation in the presence of 10 μM DPI, and after preincubation with 10 μM DPI. (**B**) Quantification of p65–eGFP distribution under control conditions, after stimulation with 4000 pulses at 50 Hz, and after stimulation in the presence of 10 mM NAC. (**C**) Quantification of p65–eGFP under control conditions, after stimulation with 4000 pulses at 10 Hz, and after the same stimulation in the presence of 10 mM NAC. Data represent mean ± SEM of the fluorescence ratio nucleus/cytoplasm from three independent experiments. Statistical significance was evaluated by one-way ANOVA followed by Bonferroni's post-test. *$p < 0.05$, **$p < 0.01$, ***$p < 0.001$.
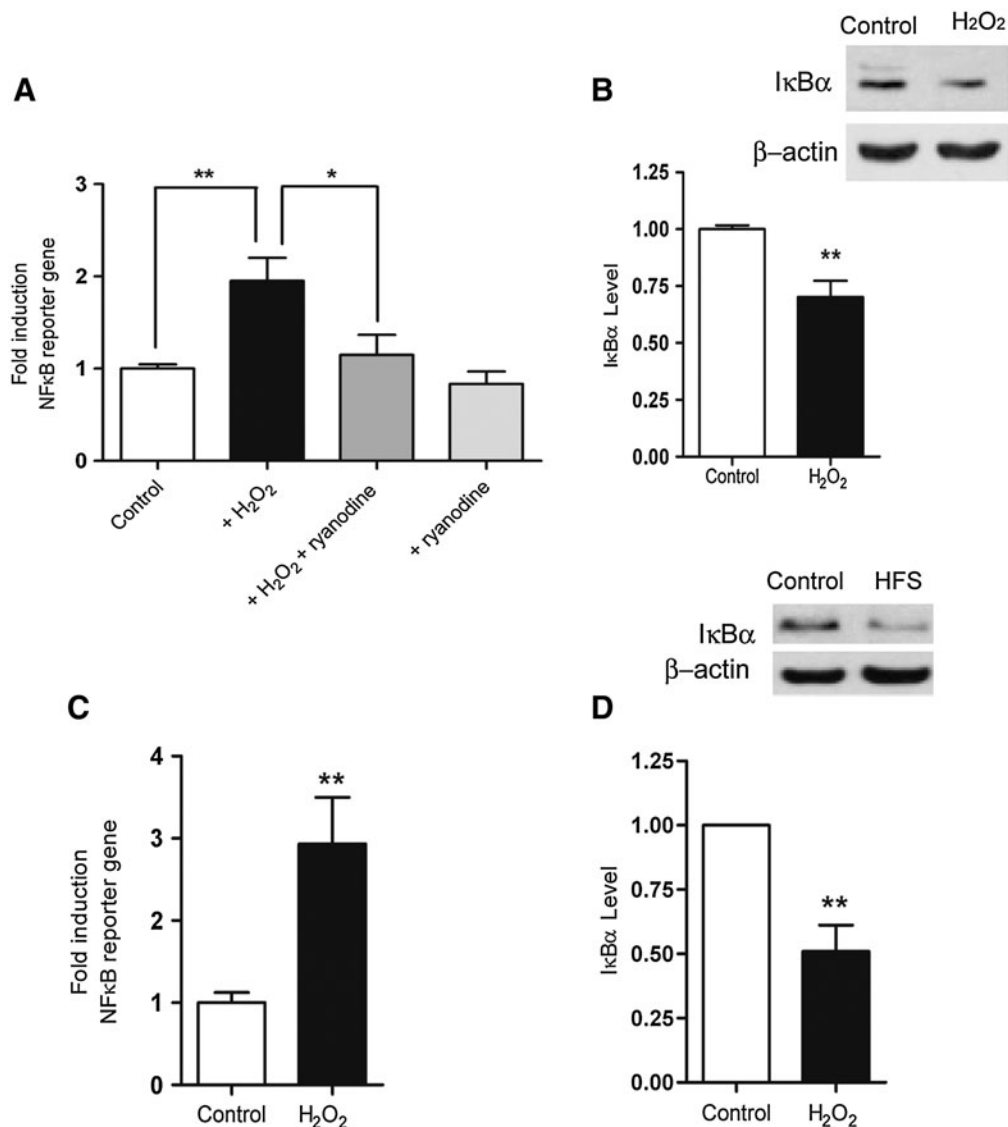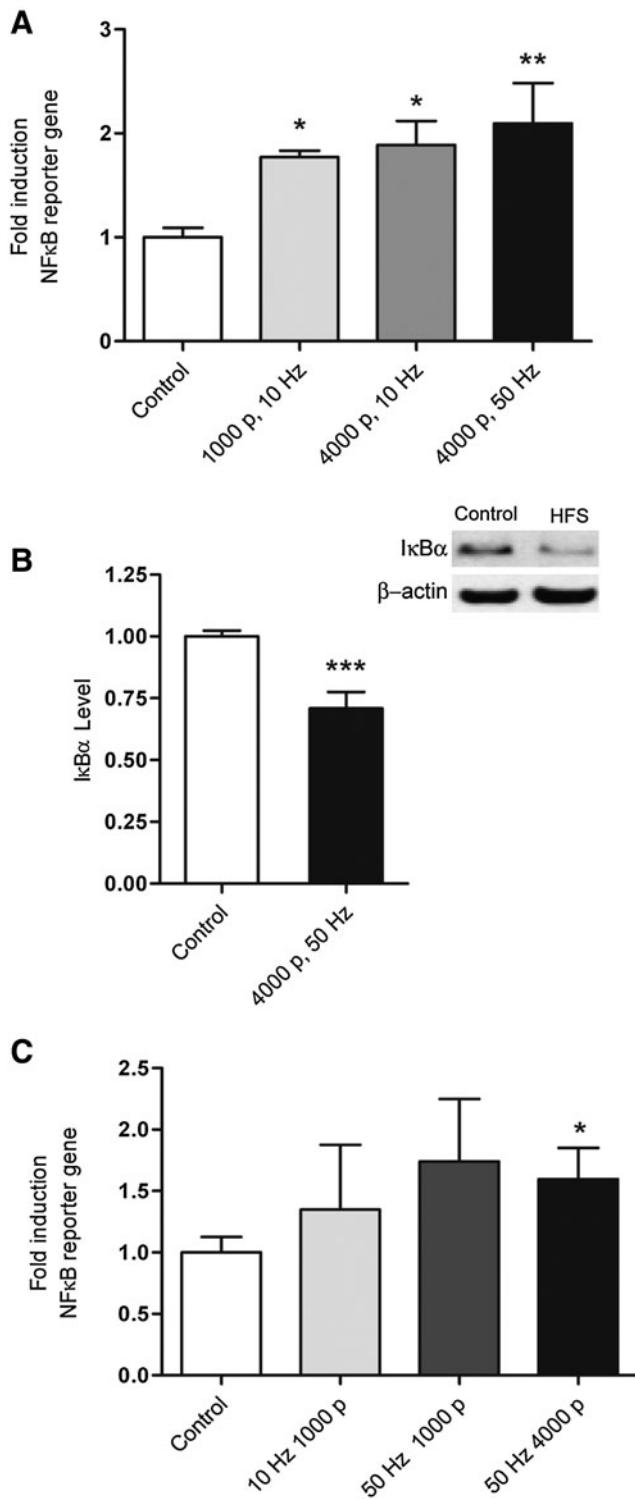
FIG. 5.   NF-κB activation in hippocampal and cortical cells exposed to exogenous H_2O_2. Hippocampal (10–13 DIV) or cortical (6 DIV) cultures were transfected with the NF-κB reporter gene and were exposed 24 h later to 200 μM H_2O_2 for 5 min. Cells were lysed 6 h after H_2O_2 addition to measure luminescence, as described in the text. Western blot determination of IκBα was performed in total cell lysates obtained 30 min after H_2O_2 treatment. (**A**) NF-κB reporter gene activity in hippo-campal cells under control conditions, exposed to 200 μM H_2O_2, exposed to 200 μM H_2O_2 after preincubation with 50 μM ryanodine, or preincubated with 50 μM ryanodine ($n = 3$). (**B**) Levels of IκBα in hippocampal cells determined by Western blot, under control conditions or following exposure to 200 μM H_2O_2 for 5 min ($n = 3$). A representative Western blot is shown next to the graph. (**C**) NF-κB reporter gene activity in cortical cells under control conditions or exposed to 200 μM H_2O_2 ($n = 3$). (**D**) Quantification of IκBα in cortical cells ($n = 3$); a representative Western blot is also shown. Bars represent mean $\pm$ SEM. Statistical significance was evaluated in **A** by two-way ANOVA followed by Bonferroni's post-test. Results in **B**, **C**, and **D** were evaluated by Student's t test. *$p < 0.05$, **$p < 0.01$.

6 h (Fig. 7) without affecting RyR2 mRNA levels (Supplemental Fig. 5). Primary hippocampal neurons preincubated with 10 mM NAC for 1 h displayed a significant decrease in RyR2 protein after HF stimulation (Fig. 7), strongly suggesting that this increase is ROS dependent.

Discussion

Electrical stimulation of neuronal cells enhances ROS generation (40, 46). It also triggers calcium-dependent signaling cascades that promote activity-induced gene expression, a key feature of synaptic plasticity, memory, and learning (11, 25, 29, 34). Together with other transcriptional regulators, the calcium- and redox-sensitive transcription factor NF-κB plays significant roles in synaptic plasticity (3, 42, 43, 54, 63), among other neuronal functions (12, 35, 76). Accordingly, one of the main objectives of this work was to study the effects of HF stimulation of primary neurons on NF-κB activity. Additionally, we investigated the specific sources of ROS and Ca^{2+} signals induced by HF stimulation, as well as their respective involvement on NF-κB activation.

FIG. 6. NF-κB activation in hippocampal and cortical cells exposed to different electrical stimulation protocols. (A) NF-κB reporter gene activity in hippocampal cells ($n = 6$–8). (B) Levels of IκBα in hippocampal cells stimulated with 4000 pulses at 50 Hz ($n = 3$), and representative Western blot of total cell lysates obtained 15 min after HF stimulation. (C) NF-κB reporter gene activity measured in cortical cells after different electrical stimulation protocols ($n = 3$). Statistical significance was evaluated in **A** and **C** by two-way ANOVA followed by Bonferroni's post-test. Results in **B** were evaluated by Student's t test. *$p < 0.05$, **$p < 0.01$, ***$p < 0.001$.
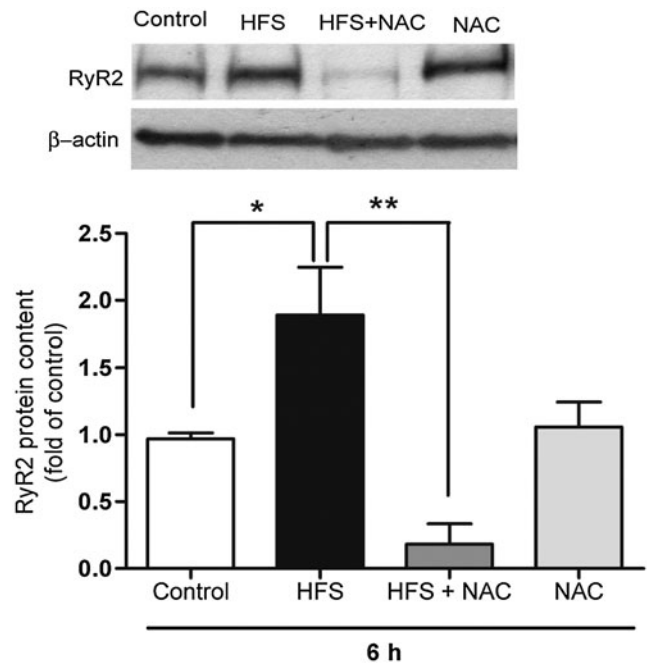
FIG. 7. RyR2 expression in electrically stimulated hippocampal cells. Control cultures or cultures preincubated with 10 mM NAC for 60 min were stimulated with 1000 pulses at 50 Hz; NAC was maintained during and after stimulation. Western blot determination of RyR2 was performed in total cell lysates obtained 6 h after stimulation. The *upper panel* illustrates a representative Western blot of RyR2 and β-actin and the *lower panel* represents the ratio between RyR2 and β-actin, normalized respect to the control values obtained in the absence of electrical stimulation and NAC. Bars represent mean ± SEM of 3–5 independent experiments. Statistical significance was evaluated by one-way ANOVA followed by Bonferroni's post-test. *$p < 0.05$, **$p < 0.01$.

Calcium and NOX-dependent ROS generation induced by HF stimulation

There is abundant literature on the functional effects of redox modifications of Ca^{2+} channels, Ca^{2+} pumps, and other molecules involved in Ca^{2+} signaling, but there is not as much information regarding the role of Ca^{2+} on ROS generation (39). A few reports indicate that neuronal activity enhances calcium-dependent ROS generation (13, 15, 31, 40). Yet we found only one report describing calcium-induced ROS formation after HF field stimulation of primary neurons (40). We deemed important to explore this response in further detail since, as mentioned above, the intracellular Ca^{2+} and ROS increases produced by strong neuronal activity play essential roles in synaptic plasticity (34, 38, 44, 46, 51).

In the present work, we confirm that primary neurons exhibit calcium-dependent ROS generation following HF stimulation, as previously reported (40). In addition, we present evidence showing that HF stimulation generates H_2O_2 via stimulation of a neuronal NOX activity. Thus, DPI when used at a concentration (0.5 μM) that specifically inhibits NOX activity without affecting mitochondrial function (1, 2) abolished H_2O_2 generation after HF stimulation. Moreover, primary hippocampal neurons containing gp91ds-tat—a peptide that inhibits NOX assembly (74)—did not generate

H_2O_2 after HF stimulation. In contrast to our findings, this previous report indicates that superoxide anion generation in primary hippocampal cells exposed to HF stimulation depends mainly on calcium-induced enhanced mitochondrial respiration (40). As a possibility to explain at least in part this apparent discrepancy, we propose that NOX-generated ROS induced by HF stimulation may promote ROS-induced ROS release from mitochondria, as described in other cell types (87). Thus, both the increase in cytoplasmic Ca^{2+} and NOX-generated ROS may jointly enhance mitochondrial ROS generation. Yet, neuronal cells must carefully control mitochondrial ROS generation since excessive ROS production would produce oxidative disease states (46). In our experiments, primary hippocampal cells remained viable after all HF stimulation protocols, showing that ROS production after HF stimulation did not reach lethal levels.

Hippocampal neurons express the NOX complex (77, 82). Moreover, NOX inhibition by pharmacologic or genetic tools prevents NMDA receptor-dependent ERK stimulation, implicating NOX in the signaling cascades that link NMDA receptors with the ERK pathway (47), an essential feature of synaptic plasticity and memory (81). Recently, Girouard et al., (31) reported that NMDA receptor activation induces ROS generation in mouse neocortex primary cells, and determined that NOX2 and neuronal nitric oxide synthase (nNOS) co-localize at postsynaptic sites with the NMDA receptor subunit NR1. These authors also showed that Ca^{2+} influx, through activated NMDA receptors, promotes nitric oxide (NO) formation by nNOS present in postsynaptic densities; in turn, NO activates NOX2 through cGMP increase and activation of cGMP-activated protein kinase (31). Thus, calcium-induced NO generation would be the intermediate link between NMDA receptor activation and NOX2-generated ROS production. Exposure of primary hippocampal neurons to NMDA also stimulates NOX-dependent ROS formation (15). The present study adds to these results by showing that HF stimulation of primary hippocampal neurons requires functional NMDA receptors to induce NOX-dependent ROS generation.

RyR-mediated Ca^{2+} release is required for ROS generation induced by HF stimulation

Calcium release from the endoplasmic reticulum participates in several neuronal signaling processes (11, 53). Increases in cytoplasmic Ca^{2+} concentration activate RyR, which are mostly responsible for the phenomenon of CICR in neurons (11, 88). In the present work, we present evidence showing that HF stimulation generated H_2O_2 via stimulation of a neuronal NOX activity, and that this response required both functional NMDA receptors and RyR-mediated Ca^{2+} release. These results indicate that ROS generation is calcium dependent, and that RyR-mediated Ca^{2+} release from the endoplasmic reticulum represents the main source of Ca^{2+} signals. Considering that inhibition of NMDA receptors with MK-801 completely blocked ROS generation, we suggest that depolarization activated-Ca^{2+} entry through post-synaptic NMDA receptors stimulates RyR-mediated Ca^{2+} release from intracellular stores, resulting in amplification and propagation of the initial Ca^{2+} entry signal via CICR (11, 20, 58). Yet, to stimulate effectively RyR-mediated CICR, concomitant ROS generation is required, as illustrated in Figure 8. The inhibitory effects of NAC on HF-induced RyR-mediated CICR agree
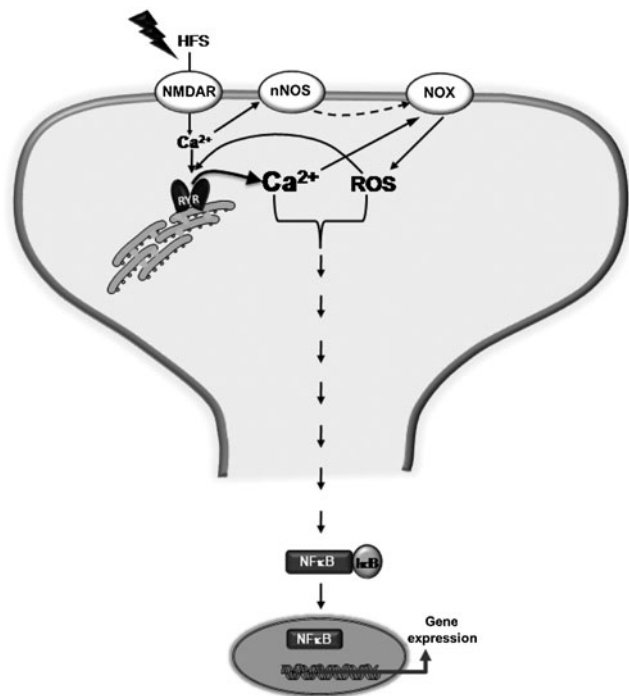
FIG. 8. **Schematic description of the pathways stimulated by HF stimulation of primary hippocampal neurons.** As indicated in the scheme, HF stimulation (HFS) of primary hippocampal neurons promotes Ca^{2+} influx through NMDA receptors (NMDAR). The resulting localized Ca^{2+} signals have two immediate targets in close proximity: nNOS and RyR (26). NOS activation, in turn, stimulates a signaling cascade that enhances NOX activity (31), leading to increased ROS generation. Activation of RyR-mediated Ca^{2+} release by Ca^{2+} requires RyR oxidation (17), which occurs through NOX-generated ROS. The amplified Ca^{2+} signals supplied by RyR (jointly activated by Ca^{2+} and ROS) further stimulate Ca^{2+}-dependent pathways that activate NOX (2). Ca^{2+}-induced NOX activation generates a positive feedback loop that leads to more ROS generation and sustained RyR-mediated Ca^{2+} signals, which propagate to the neuronal cell body and jointly promote NF-κB translocation to the nucleus. This sequence of events would explain why HFS enhanced NF-κB-dependent gene expression. In zero external Ca^{2+}, RyR activation following depolarization (see Fig. 2A) presumably takes place via mechanical coupling with L-type Ca^{2+} channels. This alternative RyR-activation pathway is not depicted in Figure 8.

with this proposal, since the redox sensitive RyR channels do not engage in CICR when highly reduced (17, 18, 52).

RyR are present throughout pyramidal CA1 neurons, including the spines and dendritic shafts (78). Synaptic stimulation of single CA1 hippocampal neurons evokes substantial RyR-mediated Ca^{2+} release from internal stores in CA1 postsynaptic spines (26). A role for RyR-mediated CICR in synaptic plasticity is emerging, and several reports have shown RyR participation in hippocampal LTP induction (9, 50, 72, 73). In addition, depletion of intracellular Ca^{2+} stores with thapsigargin or inhibition of RyR-mediated Ca^{2+} release with dantrolene significantly inhibit the release of brain-derived nerve factor (BDNF) induced by HF stimulation, suggesting that RyR-mediated CICR contributes to activity-dependent BDNF secretion (7). Recently, RyR participation in LTP

priming (59) and in a novel form of hippocampal metaplasticity has been described (75). In particular, RyR3 knockout mice exhibit reduced LTP (8, 79), and do not exhibit hippocampal superoxide-induced LTP as normal mice do, suggesting that RyR3 is particularly targeted for this effect (41).

HF stimulation stimulates NF-κB activity through RyR-mediated Ca²⁺ release and ROS generation

The increase in NF-κB activity is cell and context-dependent and occasions many functional consequences (64, 68). In mammals, the NF-κB family consists of several proteins, NF-κB1 (p50/p105), NF-κB2 (p52/p100), RelA (p65), c-Rel and RelB, which form cytoplasmic dimeric complexes. Normally, cytoplasmic NF-κB complexes are bound to IκBs, inhibitory proteins that dissociate from the NF-κB complexes in response to a number of stimuli. IκB dissociation involves sequential phosphorylation and proteolysis of IκB inhibitors by the IκB kinase (IKK) complex and the ubiquitin/proteasome system, respectively (64). Degradation of the canonical inhibitory protein IκBα, which according to our results occurs in hippocampal and cortical cells after HF stimulation or H_2O_2 addition, mainly leads to the activation of p50/p65 (64). Following IκB dissociation, the free NF-κB subunits translocate to the nucleus where they bind to target sequences in the genome. Different cytoplasmic post-translational modifications, which include phosphorylation, ubiquitination, acetylation, sumoylation, and S-nitrosylation, either inactivate the IκB inhibitory proteins or activate the NF-κB subunits directly (67). The function of NF-κB complexes is also controlled by nuclear modifications, which regulate transcriptional activity, DNA binding, and target gene specificity (23, 67). Consequently, many different factors regulate at several levels the NF-κB-dependent transcriptional response.

We found that HF stimulation (4000 pulses, at 10 or 50 Hz) of primary hippocampal neurons induced p65 nuclear translocation and NF-κB dependent transcription; nuclear translocation of p65 required ROS and RyR-mediated Ca²⁺ release from intracellular stores. The present results, showing that HF stimulation promotes calcium-dependent NF-κB activation in primary neurons, add up to previous reports describing calcium-dependent NF-κB activation (22, 49, 57). In hippocampal neurons depolarized by high K^+, NF-κB activation required subplasmalemmal Ca²⁺ increase originated from extracellular Ca²⁺ (57), but the participation of Ca²⁺ from intracellular stores was not reported. In cerebellar neurons, NF-κB activation induced by KCl-induced depolarization required mainly extracellular Ca²⁺ and a minor contribution of IP3R-mediated Ca²⁺ release (49). In striatal neurons, kainate-induced NF-κB activation requires extracellular Ca²⁺ (22). We have previously reported that NF-κB activation produced by high extracellular K^+ or HF stimulation of primary skeletal muscle cells requires both RyR- and IP3R-mediated Ca²⁺ release (83).

The transcription factor NF-κB is widely considered a ROS target; however, some authors argue that the effects of ROS on NF-κB activity are cell and context dependent (14, 66). There are a number of ROS targets at several levels of the NF-κB pathway (32, 66). These targets include IκBα, a protein amenable to ROS-induced degradation, thereby favoring NF-κB translocation to the nucleus. At the nucleus, ROS can also induce redox changes in the p65 protein, which are required for NF-κB-dependent transcription (32, 66). Reducing conditions required for NF-κB binding to DNA have also been described (32, 66).

In the present work, the complete inhibition by DPI and NAC of p65 translocation induced by HF stimulation of primary hippocampal neurons supports NOX-derived ROS involvement in this process. In addition, inhibition of RyR-mediated Ca²⁺ release prevented both ROS generation and p65 translocation. These combined observations suggest that calcium-induced ROS generation directly enhanced p65 translocation. Yet, RyR inhibition completely prevented NF-κB-mediated transcription induced by addition of exogenous H_2O_2, which in these conditions stimulates RyR-mediated Ca²⁺ release in hippocampal neurons (45). These results invoke a direct role of RyR-mediated Ca²⁺ release in the activation of NF-κB-mediated transcription produced by exogenous H_2O_2, and suggest that both ROS and RyR-mediated Ca²⁺ release are required jointly to induce NF-κB mediated transcription after HF stimulation, as detailed in Figure 8. Alternatively, exposure of neurons to exogenous H_2O_2 may not mimic effectively the highly localized and compartment specific H_2O_2 microdomains generated by different stimulation protocols (24).

The increase in RyR2 protein content caused by HF stimulation requires ROS

In addition to promoting NF-κB activation, HF stimulation produced a fast increase (45 min) in *c-fos* mRNA levels. We reported earlier that primary hippocampal neurons exposed to H_2O_2 present increased *c-fos* mRNA levels, and that this increase requires functional RyR channels (38). Thus, the increase in ROS generation and RyR-mediated CICR produced by HF stimulation may cause the observed increase in *c-fos* mRNA levels. Concurrently, 6 h after HF stimulation we observed a significant increase in RyR2 protein levels. Neurons preincubated with NAC did not present this increase but displayed a significant decrease in RyR2 protein content. Albeit there is limited information on the factors that control neuronal RyR2 expression, calcium- and ROS-dependent transcription and translation processes are likely to contribute to RyR2 protein expression in these cells.

Conclusion

The results presented here—showing NF-κB activation by HF stimulation of primary neurons—represent a novel contribution to the roles Ca²⁺ and ROS play, acting individually or jointly, on neuronal signaling pathways. Further studies to segregate pre- and post-synaptic effects of HF stimulation, plus identification of other transcriptional activators and proteins that respond to HF stimulation, should add to our current knowledge of how neurons decode HF stimulation into the expression of particular genes.

Acknowledgments

Author Disclosure Statement

No competing financial interests exist.

References

1. Abramov AY, Canevari L, and Duchen MR. Calcium signals induced by amyloid beta peptide and their consequences in neurons and astrocytes in culture. *Biochim Biophys Acta* 1742: 81–87, 2004.

2. Abramov AY and Duchen MR. The role of an astrocytic NADPH oxidase in the neurotoxicity of amyloid beta peptides. *Philos Trans R Soc Lond B Biol Sci* 360: 2309–2314, 2005.

3. Ahn HJ, Hernandez CM, Levenson JM, Lubin FD, Liou HC, and Sweatt JD. c-Rel, an NF-kappaB family transcription factor, is required for hippocampal long-term synaptic plasticity and memory formation. *Learn Mem* 15: 539–549, 2008.

4. Aracena–Parks P, Goonasekera SA, Gilman CP, Dirksen RT, Hidalgo C, and Hamilton SL. Identification of cysteines involved in S-nitrosylation, S-glutathionylation, and oxidation to disulfides in ryanodine receptor type 1. *J Biol Chem* 281: 40354–40368, 2006.

5. Aracena P, Sanchez G, Donoso P, Hamilton SL, and Hidalgo C. S-glutathionylation decreases Mg2+ inhibition and S-nitrosylation enhances Ca2+ activation of RyR1 channels. *J Biol Chem* 278: 42927–42935, 2003.

6. Balkowiec A and Katz DM. Activity-dependent release of endogenous brain-derived neurotrophic factor from primary sensory neurons detected by ELISA *in situ. J Neurosci* 20: 7417–7423, 2000.

7. Balkowiec A and Katz DM. Cellular mechanisms regulating activity-dependent release of native brain-derived neurotrophic factor from hippocampal neurons. *J Neurosci* 22: 10399–10407, 2002.

8. Balschun D, Wolfer DP, Bertocchini F, Barone V, Conti A, Zuschratter W, Missiaen L, Lipp HP, Frey JU, and Sorrentino V. Deletion of the ryanodine receptor type 3 (RyR3) impairs forms of synaptic plasticity and spatial learning. *EMBO J* 18: 5264–5273, 1999.

9. Bardo S, Cavazzini MG, and Emptage N. The role of the endoplasmic reticulum Ca2+ store in the plasticity of central neurons. *Trends Pharmacol Sci* 27: 78–84, 2006.

10. Belousov VV, Fradkov AF, Lukyanov KA, Staroverov DB, Shakhbazov KS, Terskikh AV, and Lukyanov S. Genetically encoded fluorescent indicator for intracellular hydrogen peroxide. *Nat Methods* 3: 281–286, 2006.

11. Berridge MJ. Neuronal calcium signaling. *Neuron* 21: 13–26, 1998.

12. Bhakar AL, Tannis LL, Zeindler C, Russo MP, Jobin C, Park DS, MacPherson S, and Barker PA. Constitutive nuclear factor-kappa B activity is required for central neuron survival. *J Neurosci* 22: 8466–8475, 2002.

13. Bindokas VP, Jordan J, Lee CC, and Miller RJ. Superoxide production in rat hippocampal neurons: Selective imaging with hydroethidine. *J Neurosci* 16: 1324–1336, 1996.

14. Bowie A and O'Neill LA. Oxidative stress and nuclear factor-kappaB activation: a reassessment of the evidence in the light of recent discoveries. *Biochem Pharmacol* 59: 13–23, 2000.

15. Brennan AM, Suh SW, Won SJ, Narasimhan P, Kauppinen TM, Lee H, Edling Y, Chan PH, and Swanson RA. NADPH oxidase is the primary source of superoxide induced by NMDA receptor activation. *Nat Neurosci* 12: 857–863, 2009.

16. Bull R, Finkelstein JP, Galvez J, Sanchez G, Donoso P, Behrens MI, and Hidalgo C. Ischemia enhances activation by Ca2+ and redox modification of ryanodine receptor channels from rat brain cortex. *J Neurosci* 28: 9463–9472, 2008.

17. Bull R, Finkelstein JP, Humeres A, Behrens MI, and Hidalgo C. Effects of ATP, Mg2+, and redox agents on the Ca2+

18. dependence of RyR channels from rat brain cortex. *Am J Physiol Cell Physiol* 293: C162–171, 2007.

18. Bull R, Marengo JJ, Finkelstein JP, Behrens MI, and Alvarez O. SH oxidation coordinates subunits of rat brain ryanodine receptor channels activated by calcium and ATP. *Am J Physiol Cell Physiol* 285: C119–128, 2003.

19. Caceres A, Banker G, Steward O, Binder L, and Payne M. MAP2 is localized to the dendrites of hippocampal neurons which develop in culture. *Brain Res* 315: 314–318, 1984.

20. Carrasco MA and Hidalgo C. Calcium microdomains and gene expression in neurons and skeletal muscle cells. *Cell Calcium* 40: 575–583, 2006.

21. Carrasco MA, Riveros N, Rios J, Muller M, Torres F, Pineda J, Lantadilla S, and Jaimovich E. Depolarization-induced slow calcium transients activate early genes in skeletal muscle cells. *Am J Physiol Cell Physiol* 284: C1438–1447, 2003.

22. Cruise L, Ho LK, Veitch K, Fuller G, and Morris BJ. Kainate receptors activate NF-kappaB via MAP kinase in striatal neurones. *Neuroreport* 11: 395–398, 2000.

23. Chen LF, Greene WC. Shaping the nuclear action of NF-kappaB. *Nat Rev Mol Cell Biol* 5: 392–401, 2004.

24. Davidson SM and Duchen MR. Calcium microdomains and oxidative stress. *Cell Calcium* 40: 561–574, 2006.

25. Dolmetsch R. Excitation-transcription coupling: Signaling by ion channels to the nucleus. *Sci STKE* 2003: PE4, 2003.

26. Emptage N, Bliss TV, and Fine A. Single synaptic events evoke NMDA receptor-mediated release of calcium from internal stores in hippocampal dendritic spines. *Neuron* 22: 115–124, 1999.

27. Emptage NJ, Reid CA, and Fine A. Calcium stores in hippocampal synaptic boutons mediate short-term plasticity, store-operated Ca2+ entry, and spontaneous transmitter release. *Neuron* 29: 197–208, 2001.

28. Eu JP, Sun J, Xu L, Stamler JS, and Meissner G. The skeletal muscle calcium release channel: Coupled O2 sensor and NO signaling functions. *Cell* 102: 499–509, 2000.

29. Fields RD, Lee PR, and Cohen JE. Temporal integration of intracellular Ca2+ signaling networks in regulating gene expression by action potentials. *Cell Calcium* 37: 433–442, 2005.

30. Freudenthal R, Romano A, and Routtenberg A. Transcription factor NF-kappaB activation after *in vivo* perforant path LTP in mouse hippocampus. *Hippocampus* 14: 677–683, 2004.

31. Girouard H, Wang G, Gallo EF, Anrather J, Zhou P, Pickel VM, and Iadecola C. NMDA receptor activation increases free radical production through nitric oxide and NOX2. *J Neurosci* 29: 2545–2552, 2009.

32. Gloire G and Piette J. Redox regulation of nuclear post-translational modifications during NF-kappaB activation. *Antioxid Redox Signal* 11: 2209–2222, 2009.

33. Gordeeva AV, Zvyagilskaya RA, and Labas YA. Cross-talk between reactive oxygen species and calcium in living cells. *Biochemistry (Mosc)* 68: 1077–1080, 2003.

34. Greer PL and Greenberg ME. From synapse to nucleus: Calcium-dependent gene transcription in the control of synapse development and function. *Neuron* 59: 846–860, 2008.

35. Gutierrez H, Hale VA, Dolcet X, and Davies A. NF-kappaB signalling regulates the growth of neural processes in the developing PNS and CNS. *Development* 132: 1713–1726, 2005.

36. Hernandez–Fonseca K, Cardenas–Rodriguez N, Pedraza–Chaverri J, and Massieu L. Calcium-dependent production of reactive oxygen species is involved in neuronal damage

induced during glycolysis inhibition in cultured hippocampal neurons. *J Neurosci Res* 86: 1768–1780, 2008.

37. Hidalgo C. Calcium signaling: A universal mechanism of cellular communication. *Biol Res* 37: 495, 2004.

38. Hidalgo C, Carrasco MA, Munoz P, and Nunez MT. A role for reactive oxygen/nitrogen species and iron on neuronal synaptic plasticity. *Antioxid Redox Signal* 9: 245–255, 2007.

39. Hidalgo C and Donoso P. Crosstalk between calcium and redox signaling: From molecular mechanisms to health implications. *Antioxid Redox Signal* 10: 1275–1312, 2008.

40. Hongpaisan J, Winters CA, and Andrews SB. Strong calcium entry activates mitochondrial superoxide generation, upregulating kinase signaling in hippocampal neurons. *J Neurosci* 24: 10878–10887, 2004.

41. Huddleston AT, Tang W, Takeshima H, Hamilton SL, and Klann E. Superoxide-induced potentiation in the hippocampus requires activation of ryanodine receptor type 3 and ERK. *J Neurophysiol* 99: 1565–1571, 2008.

42. Kaltschmidt B and Kaltschmidt C. NF-kappaB in the nervous system. *Cold Spring Harb Perspect Biol* 1: a001271, 2009.

43. Kaltschmidt B, Ndiaye D, Korte M, Pothion S, Arbibe L, Prullage M, Pfeiffer J, Lindecke A, Staiger V, Israel A, Kaltschmidt C, and Memet S. NF-kappaB regulates spatial memory formation and synaptic plasticity through protein kinase A/CREB signaling. *Mol Cell Biol* 26: 2936–2946, 2006.

44. Kamsler A and Segal M. Hydrogen peroxide as a diffusible signal molecule in synaptic plasticity. *Mol Neurobiol* 29: 167–178, 2004.

45. Kemmerling U, Munoz P, Muller M, Sanchez G, Aylwin ML, Klann E, Carrasco MA, and Hidalgo C. Calcium release by ryanodine receptors mediates hydrogen peroxide-induced activation of ERK and CREB phosphorylation in N2a cells and hippocampal neurons. *Cell Calcium* 41: 491–502, 2007.

46. Kishida KT and Klann E. Sources and targets of reactive oxygen species in synaptic plasticity and memory. *Antioxid Redox Signal* 9: 233–244, 2007.

47. Kishida KT, Pao M, Holland SM, and Klann E. NADPH oxidase is required for NMDA receptor-dependent activation of ERK in hippocampal area CA1. *J Neurochem* 94: 299–306, 2005.

48. Lange S, Heger J, Euler G, Wartenberg M, Piper HM, and Sauer H. Platelet-derived growth factor BB stimulates vasculogenesis of embryonic stem cell-derived endothelial cells by calcium-mediated generation of reactive oxygen species. *Cardiovasc Res* 81: 159–168, 2009.

49. Lilienbaum A and Israel A. From calcium to NF-kappa B signaling pathways in neurons. *Mol Cell Biol* 23: 2680–2698, 2003.

50. Lu YF and Hawkins RD. Ryanodine receptors contribute to cGMP-induced late-phase LTP and CREB phosphorylation in the hippocampus. *J Neurophysiol* 88: 1270–1278, 2002.

51. Lynch MA. Long-term potentiation and memory. *Physiol Rev* 84: 87–136, 2004.

52. Marengo JJ, Hidalgo C, and Bull R. Sulfhydryl oxidation modifies the calcium dependence of ryanodine-sensitive calcium channels of excitable cells. *Biophys J* 74: 1263–1277, 1998.

53. Mattson MP, LaFerla FM, Chan SL, Leissring MA, Shepel PN, and Geiger JD. Calcium signaling in the ER: Its role in neuronal plasticity and neurodegenerative disorders. *Trends Neurosci* 23: 222–229, 2000.

54. Mattson MP and Meffert MK. Roles for NF-kappaB in nerve cell survival, plasticity, and disease. *Cell Death Differ* 13: 852–860, 2006.

55. Meberg PJ, Kinney WR, Valcourt EG, and Routtenberg A. Gene expression of the transcription factor NF-kappa B in hippocampus: Regulation by synaptic activity. *Brain Res Mol Brain Res* 38: 179–190, 1996.

56. Meffert MK and Baltimore D. Physiological functions for brain NF-kappaB. *Trends Neurosci* 28: 37–43, 2005.

57. Meffert MK, Chang JM, Wiltgen BJ, Fanselow MS, and Baltimore D. NF-kappa B functions in synaptic signaling and behavior. *Nat Neurosci* 6: 1072–1078, 2003.

58. Meldolesi J. Rapidly exchanging Ca2+ stores in neurons: Molecular, structural and functional properties. *Prog Neurobiol* 65: 309–338, 2001.

59. Mellentin C, Jahnsen H, and Abraham WC. Priming of long-term potentiation mediated by ryanodine receptor activation in rat hippocampal slices. *Neuropharmacology* 52: 118–125, 2007.

60. Mermelstein PG, Bito H, Deisseroth K, and Tsien RW. Critical dependence of cAMP response element-binding protein phosphorylation on L-type calcium channels supports a selective response to EPSPs in preference to action potentials. *J Neurosci* 20: 266–273, 2000.

61. Müller M, Cheung K-H and Foskett JK. Enhanced ROS generation mediated by Alzheimer's disease presenilin regulation of InsP$_3$R Ca^{2+} signaling. *Antioxid Redox Signal* 14: 1225–1235, 2011.

62. Nelson G, Paraoan L, Spiller DG, Wilde GJ, Browne MA, Djali PK, Unitt JF, Sullivan E, Floettmann E, and White MR. Multi-parameter analysis of the kinetics of NF-kappaB signalling and transcription in single living cells. *J Cell Sci* 115: 1137–1148, 2002.

63. O'Mahony A, Raber J, Montano M, Foehr E, Han V, Lu SM, Kwon H, LeFevour A, Chakraborty–Sett S, and Greene WC. NF-kappaB/Rel regulates inhibitory and excitatory neuronal function and synaptic plasticity. *Mol Cell Biol* 26: 7283–7298, 2006.

64. Oeckinghaus A and Ghosh S. The NF-kappaB family of transcription factors and its regulation. *Cold Spring Harb Perspect Biol* 1: a000034, 2009.

65. Okubo Y, Kanemaru K, and Iino M. Imaging of Ca^{2+} and related signaling molecules and investigation of their functions in the brain. *Antioxid Redox Signal* 14: 1303–1314, 2011.

66. Oliveira–Marques V, Marinho HS, Cyrne L, and Antunes F. Role of hydrogen peroxide in NF-kappaB activation: From inducer to modulator. *Antioxid Redox Signal* 11: 2223–2243, 2009.

67. Perkins ND. Post-translational modifications regulating the activity and function of the nuclear factor kappa B pathway. *Oncogene* 25: 6717–6730, 2006.

68. Perkins ND and Gilmore TD. Good cop, bad cop: The different faces of NF-kappaB. *Cell Death Differ* 13: 759–772, 2006.

69. Pessah IN, Kim KH, and Feng W. Redox sensing properties of the ryanodine receptor complex. *Front Biosci* 7: a72–79, 2002.

70. Pfaffl MW. A new mathematical model for relative quantification in real-time RT-PCR. *Nucleic Acids Res* 29: e45, 2001.

71. Ramirez OA, Vidal RL, Tello JA, Vargas KJ, Kindler S, Hartel S, and Couve A. Dendritic assembly of heteromeric gamma-aminobutyric acid type B receptor subunits in hippocampal neurons. *J Biol Chem* 284: 13077–13085, 2009.

72. Raymond CR and Redman SJ. Different calcium sources are narrowly tuned to the induction of different forms of LTP. *J Neurophysiol* 88: 249–255, 2002.

73. Raymond CR and Redman SJ. Spatial segregation of neuronal calcium signals encodes different forms of LTP in rat hippocampus. *J Physiol* 570: 97–111, 2006.

74. Rey FE, Cifuentes ME, Kiarash A, Quinn MT, and Pagano PJ. Novel competitive inhibitor of NAD(P)H oxidase assembly attenuates vascular O(2)(-) and systolic blood pressure in mice. *Circ Res* 89: 408–414, 2001.

75. Sajikumar S, Li Q, Abraham WC, and Xiao ZC. Priming of short-term potentiation and synaptic tagging/capture mechanisms by ryanodine receptor activation in rat hippocampal CA1. *Learn Mem* 16: 178–186, 2009.

76. Sanchez–Ponce D, Tapia M, Munoz A, and Garrido JJ. New role of IKK alpha/beta phosphorylated I kappa B alpha in axon outgrowth and axon initial segment development. *Mol Cell Neurosci* 37: 832–844, 2008.

77. Serrano F, Kolluri NS, Wientjes FB, Card JP, and Klann E. NADPH oxidase immunoreactivity in the mouse brain. *Brain Res* 988: 193–198, 2003.

78. Sharp AH, McPherson PS, Dawson TM, Aoki C, Campbell KP, and Snyder SH. Differential immunohistochemical localization of inositol 1,4,5-trisphosphate- and ryanodine-sensitive Ca2+ release channels in rat brain. *J Neurosci* 13: 3051–3063, 1993.

79. Shimuta M, Yoshikawa M, Fukaya M, Watanabe M, Takeshima H, and Manabe T. Postsynaptic modulation of AMPA receptor-mediated synaptic responses and LTP by the type 3 ryanodine receptor. *Mol Cell Neurosci* 17: 921–930, 2001.

80. Starkov AA, Polster BM, and Fiskum G. Regulation of hydrogen peroxide production by brain mitochondria by calcium and Bax. *J Neurochem* 83: 220–228, 2002.

81. Sweatt JD. Mitogen-activated protein kinases in synaptic plasticity and memory. *Curr Opin Neurobiol* 14: 311–317, 2004.

82. Tejada–Simon MV, Serrano F, Villasana LE, Kanterewicz BI, Wu GY, Quinn MT, and Klann E. Synaptic localization of a functional NADPH oxidase in the mouse hippocampus. *Mol Cell Neurosci* 29: 97–106, 2005.

83. Valdes JA, Hidalgo J, Galaz JL, Puentes N, Silva M, Jaimovich E, and Carrasco MA. NF-kappaB activation by depolarization of skeletal muscle cells depends on ryanodine and IP3 receptor-mediated calcium signals. *Am J Physiol Cell Physiol* 292: C1960–1970, 2007.

84. Vertes RP. Interactions among the medial prefrontal cortex, hippocampus and midline thalamus in emotional and cognitive processing in the rat. *Neuroscience* 142: 1–20, 2006.

85. Yan Y, Wei CL, Zhang WR, Cheng HP, and Liu J. Cross-talk between calcium and reactive oxygen species signaling. *Acta Pharmacol Sin* 27: 821–826, 2006.

86. Zhao W, Meiri N, Xu H, Cavallaro S, Quattrone A, Zhang L, and Alkon DL. Spatial learning induced changes in expression of the ryanodine type II receptor in the rat hippocampus. *FASEB J* 14: 290–300, 2000.

87. Zorov DB, Juhaszova M, and Sollott SJ. Mitochondrial ROS-induced ROS release: An update and review. *Biochim Biophys Acta* 1757: 509–517, 2006.

88. Zucchi R and Ronca–Testoni S. The sarcoplasmic reticulum Ca2+ channel/ryanodine receptor: Modulation by endogenous effectors, drugs and disease states. *Pharmacol Rev* 49: 1–51, 1997.

89. Zündorf G and Reiser G. Calcium dysregulation and homeostasis of neural calcium in the molecular mechanisms of neurodegenerative diseases provide multiple targets for neuroprotection. *Antioxid Redox Signal* 14: 1275–1288, 2011.

Address correspondence to:
Prof. Cecilia Hidalgo
Facultad de Medicina
Centro de Estudios Moleculares de la Célula
and Programa de Fisiología y Biofísica
Instituto de Ciencias Biomédicas
Universidad de Chile
Independencia 1027
838-0453 Santiago
Chile

E-mail: chidalgo@med.uchile.cl

Abbreviations Used

CICR = calcium-induced calcium release
CREB = cAMP response element-binding protein
DIV = days *in vitro*
DMEM = Dulbecco's modified Eagle's medium
DPI = diphenyliodonium
ERK1/2 = extracellular-signal related kinases 1/2
GFAP = glial fibrillary acidic protein
HF = high frequency
IκBα = inhibitory NF-κB alpha
IP3R = inositol 1,4,5-trisphosphate receptor
LTP = long-term potentiation
MAP-2 = microtubule-associated protein 2
NAC = N-acetyl-L-cysteine
nNOS = neuronal nitric oxide synthase
NMDA = N-methyl D-aspartate
NO = nitric oxide
NOX = NADPH oxidase
ROI = region of interest
RyR = ryanodine receptor